

Calibrations of the LHD Thomson scattering system

Cite as: Rev. Sci. Instrum. **87**, 11E531 (2016); <https://doi.org/10.1063/1.4961276>

Submitted: 02 June 2016 • Accepted: 01 August 2016 • Published Online: 14 November 2016

 I. Yamada, H. Funaba,  R. Yasuhara, et al.



View Online



Export Citation



CrossMark

ARTICLES YOU MAY BE INTERESTED IN

[Design and performance of the Thomson scattering diagnostic on LHD](#)

Review of Scientific Instruments **72**, 1122 (2001); <https://doi.org/10.1063/1.1319368>

[The Thomson scattering system at Wendelstein 7-X](#)

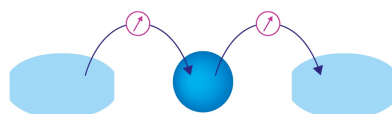
Review of Scientific Instruments **87**, 11E729 (2016); <https://doi.org/10.1063/1.4962248>

[High resolution Thomson scattering for Joint European Torus \(JET\)](#)

Review of Scientific Instruments **75**, 3891 (2004); <https://doi.org/10.1063/1.1787922>

Webinar

Interfaces: how they make
or break a nanodevice



March 29th – Register now



Zurich
Instruments

Calibrations of the LHD Thomson scattering system

I. Yamada,^{1,a)} H. Funaba,¹ R. Yasuhara,¹ H. Hayashi,¹ N. Kenmochi,¹ T. Minami,² M. Yoshikawa,³ K. Ohta,³ J. H. Lee,⁴ and S. H. Lee⁴

¹High-Temperature Plasma Physics Research Division, National Institute for Fusion Science, Toki 509-5292, Japan

²Institute of Advanced Energy, Kyoto University, Gokasho, Uji, Kyoto 611-0011, Japan

³Plasma Research Center, University of Tsukuba, Tsukuba 305-8577, Japan

⁴KSTAR Research Center, National Fusion Research Institute, Daejeon 305-806, South Korea

(Presented 8 June 2016; received 2 June 2016; accepted 1 August 2016;

published online 22 August 2016)

The Thomson scattering diagnostic systems are widely used for the measurements of absolute local electron temperatures and densities of fusion plasmas. In order to obtain accurate and reliable temperature and density data, careful calibrations of the system are required. We have tried several calibration methods since the second LHD experiment campaign in 1998. We summarize the current status of the calibration methods for the electron temperature and density measurements by the LHD Thomson scattering diagnostic system. Future plans are briefly discussed. *Published by AIP Publishing.* [<http://dx.doi.org/10.1063/1.4961276>]

I. LHD THOMSON SCATTERING SYSTEM

The Large Helical Device (LHD) Thomson scattering system measures electron temperature (T_e) and density (n_e) profiles of LHD plasmas along the LHD major radius at a horizontally elongated section.^{1–3} Figure 1 shows the schematic diagram of the LHD Thomson scattering system, and the typical specifications are summarized in Table I. In typical LHD experiments, we measure T_e and n_e in 144 spatial points, which cover the entire core plasma region of LHD plasmas. Temporal sampling frequency is determined by the laser repetition rate. Currently, four neodymium-doped yttrium-aluminum-garnet (Nd:YAG) lasers are available: one 1.6 J-30 Hz laser (Continuum DLS 9030), two 2 J-10 Hz lasers (Thales SAGA 230-10), and one 0.55 J-50 Hz laser (Continuum NY-8050). Therefore, measurements at the sampling frequency of 10–100 Hz are possible. The LHD Thomson scattering system observes backscattering light as shown in Fig. 1, and the typical scattering angle is 167° . Thomson scattered light is collected by a large spherical mirror on the optical fibers of which the core diameter, numerical aperture (NA), and length are 2.0 mm, 0.2, and 40 m, respectively. The Thomson scattered light is transmitted to 144 polychromators through the fibers. Each polychromator has five wavelength channels used for the Thomson scattering diagnostic and is equipped with an additional channel used for Rayleigh scattering calibrations. We determine T_e and n_e by using the lookup table method and minimum χ^2 method. Thomson scattering spectra used in the analysis are calculated by using the modified Selden's formula.^{4,5}

II. CALIBRATION FOR T_e MEASUREMENT

Since T_e is determined from the wavelength distribution of the Thomson scattering spectrum, the calibration of the wavelength dependences of the spectral responses of polychromator channels is one of the most important issues. We determine the spectral response curves of polychromators by using a monochromatized light source. The light from a halogen lamp is monochromatized by a Czerny-Turner grating monochromator (CVI DK240), of which the focal length and effective aperture ratio are 240 mm and $f/3.9$, respectively. The wavelength of the monochromator is calibrated by using a low-power continuum YAG laser, He–Ne laser, and mercury lamp. The wavelength dependence of the output intensity is calibrated by using some calibrated Si photodiodes (Melles Griot: D99G0299 and Thorlabs: FDS100CAL) for which the absolute spectral responsivity data are provided for each product. We carefully measured the output spectrum by using the detectors. Figure 2 shows the output intensity spectrum determined by the Thorlabs photodiodes together with the spectral responsivity. The uncertainty of the output intensity has been estimated to be 3% by comparing the data obtained by some photodiodes. The uncertainty is taken into account in T_e and n_e analysis. The experimental error in T_e and n_e due to the uncertainty of the output spectrum is estimated to be less than 2%. We have carried out the polychromator calibration every year before experiment campaigns. The spectral responses of a polychromator, $f_i(\lambda)$, measured in 2007–2014 are overplotted in Fig. 3(a). We made a major improvement for all polychromators in 2006–2007, in which the installation of Rayleigh scattering channel and related works were completed. Therefore, it may be meaningless to directly compare the spectral response data measured before and after 2007. Figure 3(b) shows the history of the integral values of each wavelength channel, $\int f_i(\lambda) d\lambda$, obtained in 2007–2014. No significant and/or systematic variations are

Note: Contributed paper, published as part of the Proceedings of the 21st Topical Conference on High-Temperature Plasma Diagnostics, Madison, Wisconsin, USA, June 2016.

^{a)}Author to whom correspondence should be addressed. Electronic mail: yamadai@nifs.ac.jp.

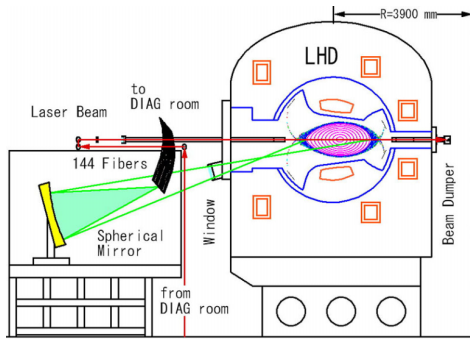


FIG. 1. Schematics of the LHD Thomson scattering.

seen, and the typical variations are less than 5%. The room temperature of our laboratory is kept within $\pm 0.5^\circ$, and the humidity is also well controlled. Therefore, we consider that the degradation of the performance of our polychromators is small, and annual calibration is sufficient.

Concerning the wavelength dependences of the observation window transmittance, light collection mirror reflectivity, and fiber transmittance, these are also important. We measured them by using a small halogen lamp and mini spectrometer. However, satisfactory calibration data were not obtained because the sensitivity of our spectrometer near the laser wavelength, 1064 nm, is too low. Currently we do not take these wavelength dependences into account in T_e and n_e analysis. However, the error due to neglecting these wavelength dependences was estimated to be less than 1% at $T_e \leq 5$ keV, 2% at $T_e = 5$ -10 keV, and 5% at $T_e = 10$ -20 keV. We will remeasure the wavelength dependences by using new spectrometers whose sensitivity near the laser wavelength is 3-5 times higher than the old spectrometer in the near future.

III. CALIBRATION FOR n_e MEASUREMENT

In Thomson scattering diagnostic, electron densities are determined from the absolute measurement of the Thomson scattered light intensity. In the LHD Thomson scattering system, Rayleigh scattering and Raman scattering in gaseous nitrogen and/or dry air have been tested for the absolute calibration.⁶ It is noted that we tried Raman scattering calibration using gaseous hydrogen for the Compact Helical System (CHS) Thomson scattering system, which was developed as a prototype of the LHD Thomson scattering system.⁷ In both the Rayleigh and Raman scattering calibrations, the LHD vacuum vessel is filled with target gas up to about 30-50 kPa. The target gas density is determined by using a state equation of ideal gas. The gas temperature and pressure are monitored

TABLE I. Specifications of the LHD Thomson scattering system.

	Outside-inside	Units
Scattering angle	161-171	(deg)
Solid angle	39.0-9.4	(msr)
Spatial resolution	11.6-25.4	(mm)
Number of spatial points	144	...
Sampling frequency	10-100	(Hz)
Measurable T_e range	5-20 000	(eV)
Measurable n_e range	$\geq 10^{18}$	(m^{-3})

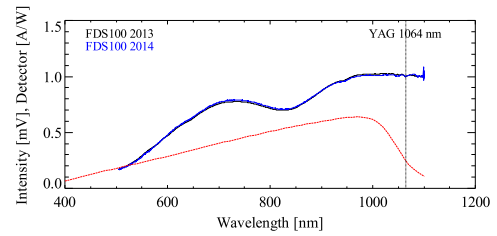


FIG. 2. Solid curves show the monochromator output intensity. Dotted curve shows the spectral responsivity of calibrated Si photodiode (Thorlabs FDS100CAL).

by a thermocouple sensor installed inside the vacuum vessel and a capacitance manometer that can measure absolute gas pressure, respectively. The Raman scattering calibration is carried out under the same settings of the laser system as the Thomson scattering measurements. On the other hand, laser pulse energy is decreased about 1/100-1/1000 in Rayleigh scattering calibration, because the Rayleigh scattering cross section is three orders of magnitude larger than the Raman scattering cross sections. Stray light intensity is also decreased in proportion to laser pulse energy. Then, stray light effect does not cause a serious problem though non-negligible stray light is observed in our Rayleigh scattering calibrations. Figure 4 shows an example of the target gas pressure dependence of measured signal intensity. The Rayleigh scattering signal intensity is proportional to the gas pressure, as expected. It is noted that Rayleigh scattering has the same scattering properties as Thomson scattering because both of them are generated from dipole transition. On the other hand, since Raman scatterings are quadrupole transitions, the angular distribution of emitted light should be taken into account.

In our calibration experiments, Rayleigh scattering calibration has been found to provide better results than Raman scattering calibration because the spectral response of the polychromators at the Rayleigh scattering wavelength (=incident laser wavelength) can be more accurately determined in our polychromators. In order to verify the reliability of the Rayleigh scattering calibration, we compared line-integrated

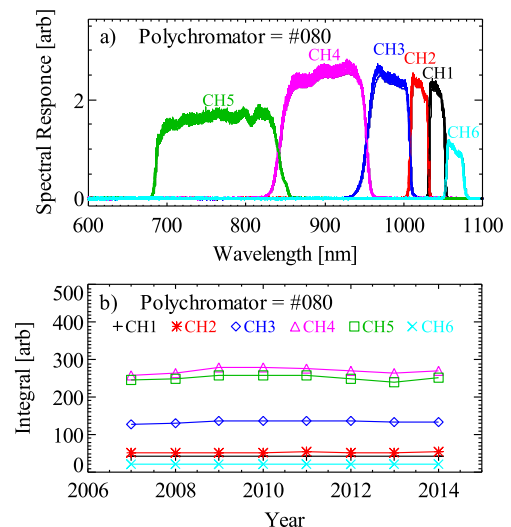


FIG. 3. (a) Spectral responses measured in 2007-2014. The CH. 6 is used for the Rayleigh scattering calibration and not used for Thomson scattering measurement. (b) The history of the integral value for each wavelength channel.

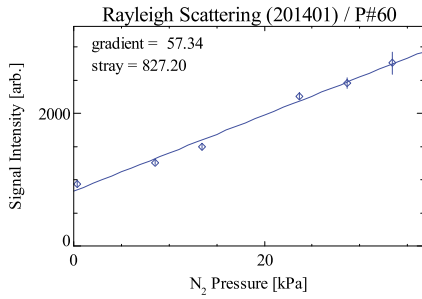


FIG. 4. Signal intensity as a function of target gas pressure in Rayleigh scattering calibration.

electron densities obtained from the Thomson scattering diagnostic to those obtained by the LHD millimeter-wave (MMW) interferometer diagnostic.⁸ Both of the two diagnostic systems measure electron density along the LHD major radius at a horizontally elongated section. Thus, the two results can be directly compared without any assumption and/or special procedure such as the Abel inversion. Figure 5(a) shows an example of the comparison for an LHD plasma discharge, showing good agreement. Figure 5(b) shows the summary of the comparison for the data obtained in the latest, 2014 LHD experiment campaign. The horizontal axis is the LHD discharge number. Roughly speaking, they show good agreements throughout the campaign of 3 months. The systematic error is estimated to be +4.3%. And, it is found that the ratio is slightly decreased in the campaign. We are considering that it is due to the long-term variation of the laser pulse energy. We have monitored the laser pulse energy for all laser pulses, however, the reliability of the laser energy monitor system may not be satisfactory. We must replace it with a better system to obtain more accurate density data.

IV. CALIBRATION FOR MEASUREMENT POINT

Thomson scattering diagnostic system measures local T_e and n_e . Thus, the information of the measurement points is

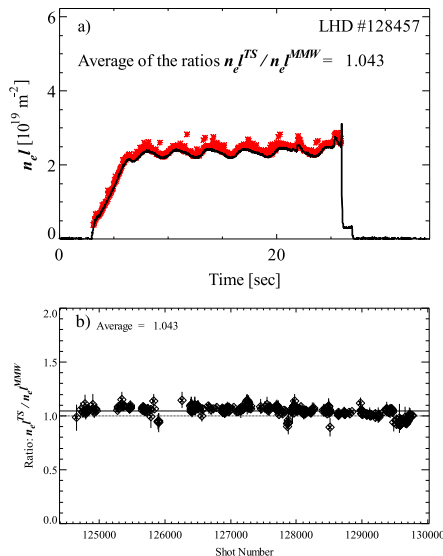


FIG. 5. (a) Comparison of line-integrated electron densities obtained by the LHD Thomson scattering (crosses) and MMW interferometer (solid curve) diagnostics. (b) Summary of the comparison in the 2014 experiment campaign.

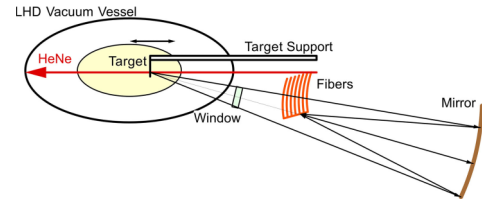


FIG. 6. Schematic diagram of the calibration of measurement point.

also important. In the usual YAG Thomson scattering systems, each fiber and its measurement point are in one-to-one correspondence. We calibrate the measurement point observed by each fiber by a simple process. First, a reference He–Ne laser beam is injected into the LHD vacuum vessel, such as the YAG laser. Then, a linearly movable target plate is also introduced into the vacuum vessel from another port, as shown in Fig. 6. By scanning the target along the laser beam (i.e., the LHD major radius), we obtain the one-to-one correspondence table for the fiber number and observation position. The position calibration is carried out before the experiment campaign when the environment at the inside of the vacuum vessel is an atmospheric air open state. We are now installing a new target driving system. The system can be operated even when the vacuum vessel is evacuated and has a precise remote control system. The uncertainty in the previous target scanning method is estimated to be 10 mm in the worst case because the target support structure and scanning method are poor. By using the improved target scanning system, the uncertainty will be decreased down to 1 mm.

V. SUMMARY

We installed the LHD Thomson scattering system in 1998 and have tried some calibration methods to obtain accurate and reliable T_e and n_e profiles. We summarized the current status of some calibration methods used in the LHD Thomson scattering diagnostic. Calibration systems using new instruments and/or an improved system will provide more accurate calibration data.

ACKNOWLEDGMENTS

This work was supported by the NIFS LHD project budgets (Grant Nos. NIFS14ULHH005 and NIFS15ULHH005), JSPS KAKENHI Grant No. 25289341, and Japan-Korea KSTAR diagnostics collaboration program (KpHDJ-01).

- ¹K. Narihara, K. Yamauchi, I. Yamada, T. Minami *et al.*, *Fusion Eng. Des.* **34–35**, 67 (1997).
- ²K. Narihara, I. Yamada, H. Hayashi, and K. Yamauchi, *Rev. Sci. Instrum.* **72**, 1122 (2001).
- ³I. Yamada, K. Narihara, H. Funaba, T. Minami, H. Hayashi, T. Kohmoto, and LHD Experiment Group, *Fusion Sci. Technol.* **58**, 345 (2010), http://www.ans.org/pubs/journals/fst/a_10820.
- ⁴A. C. Selden, *Phys. Lett. A* **79**, 405 (1980).
- ⁵I. Yamada, R. Yasuhara, H. Funaba, K. Narihara *et al.*, in *Proceedings 40th EPS Conference Controlled Fusion Plasma Physics, Espoo, Finland, 1–5 July 2013* (European Physical Society, 2013), Vol. 37D, p. O2.112.
- ⁶I. Yamada, K. Narihara, H. Hayashi, H. Funaba, and LHD Experimental Group, *Plasma Fusion Res.* **2**, S1106 (2007).
- ⁷I. Yamada, K. Narihara, T. Minami, and K. Yamauchi, NIFS Annual Report April 1994–March 1995, 1995, p. 226.
- ⁸K. Kawahata, K. Tanaka, Y. Ito, A. Ejiri, and R. J. Wylde, *Rev. Sci. Instrum.* **70**, 695 (1999).